Post-Synthetic Modification of UiO66 and its Application in Catalytic Reactions

Mingshan Qin
Tianjin Agricultural University
Juan Gao
Tianjin Agricultural University
Dongwei Wei
Tianjin Agricultural University
Liuan Li
Tianjin Agricultural University
Cun Li
Tianjin Agricultural University
Linyan Yang (y_linyan@163.com)
Tianjin Agricultural University

Research Article

Keywords: UiO66, MOFs, Modification, Knoevenagel Reaction

Posted Date: June 21st, 2021

DOI: https://doi.org/10.21203/rs.3.rs-629998/v1

Abstract

Because of their unique surface area and adjustable pore size, Metal-Organic Frameworks(MOFs) have been widely used in lots of research fields, such as catalysis, energy storage, sensing, separation. In this paper, as for the Knoevenagel reaction, UiO66 and other UiO series MOFs were synthesized and modified. UiO66 nanoparticles were prepared by one-pot method. 2-aminopyridine, 3-aminopyridine and 4-aminopyridine were used to prepare UiO66-2Py, UiO66-3Py and UiO66-4Py nanoparticles. UiO66-2Py, UiO66-3Py and UiO66-4Py nanoparticles were modified by activated arginine, lysine and glycine to synthesize UiO66-2Py-Arg, UiO66-3Py-Lys and UiO66-4Py-Gly. Finally, the obtained samples were used for the Knoevenagel catalytic condensation reactions of benzaldehyde and ethyl cyanoacetate. In this process, the prepared samples and their intermediates were characterized by infrared spectroscopy (IR) and X-ray diffraction(XRD), which showed that the modification of UiO66 was successful. UiO66-3Py-Lys and UiO66-4Py-Gly showed high catalytic activity in the supernatant determined by fluorescence spectrophotometer, and UiO66-4Py-Gly showed the best catalytic effects at the volume of 0.4mL benzaldehyde.

1. Introduction

Recently, Post-Synthesis Modification(PSM), the elaboration of a known MOF to give a series of new materials with the same structure but bearing different chemical functionalities, has been proposed as efficient and rational routes to obtain new MOFs[1]. Post-Synthesis Modification (PSM) of Metal-Organic Frameworks (MOFs) has become a useful tool to prepare functionalized MOFs for various applications, such as gas storage and separation, sensors, biosensor, drug delivery and catalysis[2]. The first generation of MOFs were formed by linking together metal centers with simple, commercially available bridging ligands, such as 1,4-benzenedicarboxylate (bdc)[3]. Among various MOFs, UiO-66 is a three-dimensional porous zirconium-based MOF assembled from a 1,4-benzenedicarboxylic linkers and a cationic $Zr_6O_4(OH)_4$ nodes, having octahedral and tetrahedral cavities[4]. Generally, the organic components of MOFs have attracted more attention for PSM via the diverse organic reaction to covalently attach organic molecules. The unsaturated sites of metal center in MOFs can be further coordinated or substituted by other molecules containing O or N atoms, such as imidazole, pyridine, and alcohol[5]. Ingleson et al have reported that postsynthetic transformation of a MOF by diamine grafting onto unsaturated metal centers introduces accessible secondary amine functionalities[6]. However, The introduction of amino-groups to the MOFs has been particularly effective and the catalytic applications of amine-functionalized IRMOF-3 or amino-MIL-53 for Knoevenagel reactions have been reported[7].

Applications of MOFs in chemical catalysis have gained interest in lots of chemical reactions, such as the Claisen-Schmidt reaction, cross-aldol condensation, ring-opening polymerization of epoxides, acetalization of aldehydes, acid-catalyzed selective hydrogenations, et al. Examples of MOFs used for chemical catalysis include Fe(BTC), UiO-66(NH_2), $Cu_3(BTC)_2$, $Cu(NO_3)_2{\cdot}3H_2O$, Al-MCM-41, et al[8]. Hwang et al. have demonstrated that ethylenediamine(ED) and diethylenetriamine(DETA) can be used as new

grafting agents to produce the amine-grafted MIL-101, exhibiting the remarkably high activities in the Knoevenagel condensation[9].

In order to investigate the effects of the Knoevenagel catalytic condensation reactions, UiO66, UiO66-2Py, UiO66-3Py, UiO66-4Py, UiO66-2Py-Arg, UiO66-3Py-Lys and UiO66-4Py-Gly nanoparticles were prepared to study catalytic activity in the supernatant determined by fluorescence spectrophotometer.

2. Experimental Section

2.1 Materials and Physical Measurements

Terephthalic acid(H_2BDC), 2-aminopyridine(2-Py), 3-aminopyridine(3-Py), 4-aminopyridine(4-Py), 1-(3-Dimethylaminopropyl)-3-ethylcarbodiimide hydrochloride (EDC), *N*-Hydroxysuccinimide (NHS), arginine(Arg), lysine(Lys) and glycine(Gly) were purchased from Shanghai source biological technology co., LTD (Shanghai, China). All commercially available chemicals and solvents were of reagent grade and used without further purification.

IR spectra were recorded in the range of 4000 – 400 cm^{-1} on a Perkin-Elmer spectrometer with KBr pellets. X-ray powder diffraction (XRD) intensities were measured on a Rigaku D/max-IIIA diffractometer (Cu-Kα, λ = 1.54056Å). Flourescence spectroscopy data could be recorded on HORIBA Jobin Yvon HJY-FL3-221-TCSPC spectrophotometer.

The catalytic data were obtained by RP-HPLC (Reversed phase high performance liquid chromatography). The HPLC system was from Agilent Technologies 1260 Infinity (Agilent Technologies, SantaClara, CA, USA), and was equipped with a quaternary pump and UV-Vis detector(Agilent Technologies). The chromatographic separation was carried out on an ACE Super C18 column(50×2.0 mm i.d., 5μm, FLM, Guangzhou, China). The mobile phase was slanted from 10–80% of acetonitrile(0.02% of trifluoroacetic acid) in the first 4 minutes, and the column was rinsed with 80% acetonitrile in the last 0.9 minutes, while the aqueous phase was 0.04% of trifluoroacetic acid. The flow rate was 0.8mL/min and the column temperature was set to 40℃. The effluent was monitored at 220nm and the injection volume was 0.2μL.

2.2 Preparation and Modification of UiO66 Nanoparticles

UiO66 nanoparticles were prepared according to the previous method[10]. UiO66 nanoparticles were dried under vacuum at 150℃ overnight, and the coordinated water could be removed to obtain activated UiO66[11].

2.2.1 Preparation of Aminopyridine Modified Nanoparticles

2-aminopyridine(2-Py)(50mg, 0.53mmol) and activated UiO66 nanoparticles(500mg) were added into 30mL of dichloromethane. The mixture was heated at 55℃ for 12h to yield aminopyridine modified products. After filtration, the product was washed by dichloromethane, and UiO66-2py nanoparticles

could be obtained via naturally dry process[12]. 2-aminopyridine(2-Py) could be replaced by 3-aminopyridine(3-Py) and 4-aminopyridine(4-Py), and UiO66-3py and UiO66-4py nanoparticles could be obtained.

2.2.2 Preparation of Amino Acid Modified Nanoparticles

An arginine(Arg) solution (2mg/mL) was converted to *N*-hydroxysuccinimide esters by sequential reaction with EDC (38.4mg/mL in MES buffer, pH 6.0) for 15 min and NHS (23mg/mL in MES buffer, pH 6.0) for 60min. The activated solution was then introduced to the obtained UiO66-2py nanoparticles(500mg in 40mL of MES buffer), and then the reaction proceeded in the shaker at 37℃ for 78h. After washing by ethanol, the samples of UiO66-2py-Arg could be obtained by vacuum-dried process at 80℃. The preparation process was the same as UiO66-2py-Arg nanoparticles, except that arginine(Arg) was replaced by lysine(Lys) and glycine(Gly). And UiO66-3Py-Lys and UiO66-4Py-Gly nanoparticles were obtained.

2.3 Knoevenagel Condensation Test

The Knoevenagel Condensation reactions between benzaldehyde(LBA) and ethyl cyanoacetate(ECA) were undertaken using UiO66-2Py-Arg, UiO66-3Py-Lys and UiO66-4Py-Gly nanoparticles as catalysts. A mixture of catalyst(0.05g) and ethyl cyanoacetate(7mmol) was added into 10mL of ethanol. After heated to boil, a series of Benzaldehyde (0.2mL, 0.4mL, 0.8mL, 1.6mL, 3.2mL) were separately added, and the reactions proceeded for 3h. After the reactions were complete, the catalysts were separated by centrifugation. The products were analyzed using fluorescence spectrophotometer(λ_{ex} = 400nm, slit = 20nm) based on benzaldehyde[13].

In order to verify the fluorescence results, RP-HPLC was used to determine part of the catalytic reaction results. Benzaldehyde(LBA, 0.8mL) was added into 10mL of ethanol, as sample 1. A mixture of benzaldehyde(0.8mL) and ethyl cyanoacetate(7mmol) was added into 10mL of ethanol, as sample 2. The reaction mixture of benzaldehyde(0.8mL), ethyl cyanoacetate(7mmol) and the best catalyst was added into 10mL of ethanol, as sample 3.

^{1}HNMR(400M Hz, $CHCl_3$-d_6) charomatogram of the reaction product could be obtained via the processes: Petroleum ether(PE) to ethyl acetate(EA)(10:1) was used as a expanding agent, and the new spots on the silicone plate were scraped off. The obtained sample was soaked in dichloromethane for 30min, and then filtrated. The filtrate was concentrated and dissolved in $CHCl_3$-d_6, and ^{1}HNMR(400M Hz) charomatogram could be measured.

3. Results And Discussion

3.1 IR Analysis

A series of products were obtained by PSM of UiO66 MOFs. Infrared Spectroscopy(IR) was used for characterization of the obtained nanoparticles. As shown in Fig. 1, the IR spectra includes the

characteristic peak of UiO66 nanoparticles at 1400cm^{-1}, and the vibration peaks were generated by the symmetric stretching of the carboxyl group due to the organic ligands in UiO66. The vibration peaks generated by the C = C bond vibration of the benzene ring in terephthalic acid were located at 1504cm^{-1} and 1587cm^{-1}. Among them, the characteristic peak at 554cm^{-1} caused by the vibration of Zr-O bonds was the strongest evidence of the successfully preparation of UiO66[14].

For UiO66-2Py, UiO66-3Py and UiO66-4Py nanoparticles, because of the newly introduced nitrogen-containing components after amination, a characteristic peak at about 2900cm^{-1} could be assigned to C-H stretching vibration peak. Because of the stretching vibration peak of the aromatic ring, its unique skeleton band could be seen at 1640 ~ 1680cm^{-1}[7, 15].

UiO66-2Py-Arg, UiO66-3Py-Lys and UiO66-4Py-Gly nanoparticles were modified by amidation and the peaks at 1640 ~ 1680cm^{-1} disappeared, while only the characteristic bands of amides could be seen[16, 17].

3.2 XRD Analysis

Figure 2 is the XRD patterns of UiO66 and the modified materials obtained by PSM. The peaks at 2θ values of 7.09°, 8.58°, 12.39°, 14.95°, 16.85°, 25.58°, 30.90°, 43.23° were resembles the diffraction spectrum of UiO66 with respect to its reflection peaks positions. The results showed that the preparation and modification of UiO66 nanoparticles were successful[18].

3.3 Knoevenagel Condensation Results

3.3.1 Fluorescence Analysis

The activity of solid base catalysts for Knoevenagel condensation could be analyzed by fluorescence and RP-HPLC. Solvent polarity has important influence on the effects of the catalytic reactions. Herein, ethanol(a protic solvent, ε = 24.3) could be used in our experiments, which has been verified by our previous experiments.

Prof. Li has reported the catalytic performance of Fe_3O_4/IRMOF-3 via the Knoevenagel condensation reaction of benzaldehyde and ethyl cyanoacetate[13].

Here, UiO66-2Py-Arg, UiO66-3Py-Lys and UiO66-4Py-Gly nanoparticles were used as catalysts for the Knoevenagel condensation reactions.

The fluorescence emission spectra of 0.8mL benzaldehyde under different catalysts were shown in Fig. 3a. The fluorescence intensity of the condensation reactions without catalysts was the highest, which was in accordance with the principle. The fluorescence intensity of the products catalyzed by UiO66-3Py-Lys and UiO66-4Py-Gly was very low, indicating that UiO66-3Py-Lys and UiO66-4Py-Gly showed better catalytic activity than that of UiO66-2Py-Arg.

As shown in Fig. 3b, in the condensation reactions with UiO66-2Py-Arg as the catalysts, when 0.4 mL of benzaldehyde was added, the fluorescence intensity was the lowest, indicating that 0.4 mL of benzaldehyde showed the best catalysis effect when the gradient volumes were used.

In order to further explore which has the best catalytic effect with 0.4mL of benzaldehyde, as shown in Fig. 3c, the results showed that the catalytic effect of UiO66-4Py-Gly with 0.4mL of benzaldehyde was the best. Although UiO66-2Py-Arg showed a good catalytic effect with 0.4mL of benzaldehyde, under the same conditions, compared with the other two UiO66-3Py-Lys and UiO66-4Py-Gly catalysts, UiO66-2Py-Arg was still unsatisfactory.

As shown in Fig. 3d, with different gradient volumes of benzaldehyde, the results showed that the catalytic effect of UiO66-3Py-Lys was the best when the benzaldehyde solution with a gradient volume of 0.8 mL.

As shown in Fig. 3e, with different gradient volumes of benzaldehyde, when UiO66-4Py-Gly was used as a catalyst, the results showed that 0.8 mL of benzaldehyde showed the best catalytic effect.

The analysis showed that, compared with UiO66-2Py-Arg, UiO66-3Py-Lys and UiO66-4Py-Gly showed better catalytic activity, which might be related to the positions of the substituents. When there is a steric hindrance factor, samples with ortho-substituents have lower selectivity and catalytic activity than those with para- or meta-substituents.

At the same time, the catalytic effects of UiO66-3Py-Lys and UiO66-4Py-Gly at a volume of 0.8mL of benzaldehyde were equivalent and the most ideal. At a volume of 0.4mL of benzaldehyde, the catalytic activity of UiO66-4Py-Gly was better than that of UiO66-3Py-Lys.

3.3.2 RP-HPLC and ^{1}HNMR Analysis

As shown in Fig. 4a, a control experiment, the retention time of diluted benzaldehyde was 1.668 min. In Fig. 4b, the retention time of the new product was 3.040min, and the area percentage was 54.033%. In Fig. 4c, the retention time of the new product was 3.034min, and the area percentage was 79.050%. Compared with UiO66-2Py-Arg and UiO66-3Py-Lys nanoparticles, in the presence of UiO66-4Py-Gly nanoparticles, the Knoevenagel condensation reaction presented much higher catalytic activity.

In Fig. 4d, the retention time of the reaction product was 3.028min. In Fig. 4e, the ^{1}HNMR(400M Hz, $CHCl_3$-d_6) charomatogram of the reaction product showed that UiO66-4Py-Gly nanoparticles presented catalytic activity.

It is noteworthy that the performance of UiO66-4Py-Gly nanoparticles was better than that of UiO66-2Py-Arg and UiO66-3Py-Lys nanoparticles. Some literatures reported amino groups might play the major role in the Knoevenagel condensation reaction, while in our experiments, a steric hindrance factor might a quite important element[19–23].

4. Conclusions

In conclusion, UiO66 nanoparticles were prepared by one-pot method. 2-aminopyridine, 3-aminopyridine and 4-aminopyridine were used to prepare UiO66-2Py, UiO66-3Py and UiO66-4Py nanoparticles. UiO66-2Py, UiO66-3Py and UiO66-4Py nanoparticles were modified by activated arginine, lysine and glycine to synthesize UiO66-2Py-Arg, UiO66-3Py-Lys and UiO66-4Py-Gly, which were used for the Knoevenagel catalytic condensation reactions of benzaldehyde and ethyl cyanoacetate. IR and XRD analysis were used for the characterizations of the prepared samples and their intermediates, which showed that the modification of UiO66 was successful. For UiO66-2Py, UiO66-3Py and UiO66-4Py nanoparticles, a characteristic peak at about 2900cm^{-1} could be assigned to C-H stretching vibration peak. As for the aromatic, the stretching vibration peak could be seen at 1640 ~ 1680cm^{-1}. UiO66-2Py-Arg, UiO66-3Py-Lys and UiO66-4Py-Gly nanoparticles were modified by amidation and the peaks at 1640 ~ 1680cm^{-1} disappeared, while only the characteristic bands of amides could be seen. The peaks of XRD were resembles the diffraction spectrum of UiO66 with respect to its reflection peaks positions. In fluorescence analysis, UiO66-3Py-Lys and UiO66-4Py-Gly showed high catalytic activity, while UiO66-4Py-Gly showed the best catalytic effects at the volume of 0.4mL benzaldehyde. While in RP-HPLC spectra, the retention time of the reaction product was 3.028min. The ^{1}HNMR(400M Hz, $CHCl_3$-d_6) charomatogram of the reaction product showed that UiO66-4Py-Gly nanoparticles presented catalytic activity. Some literatures reported amino groups might play the major role in the Knoevenagel condensation reactions, while in our experiments, a steric hindrance factor might a quite important element.

Declarations

Funding

This work was supported by Outstanding Research Achievement Award Project of Tianjin agricultural university, the Open Topic of Guangxi Key Laboratory for the Chemistry and Molecular Engineering of Medicinal Resources (CMEMR2016-B12), the National Natural Science Foundation of China (No.21875117, No.31572492), the University-level Innovative and Entrepreneurial Training Plan for College Students (202010061066), the Veterinary Biotechnology Scientific Research Innovation Team of Tianjin, China (Grant No.TD12-5019), the Veterinary “Innovative Talent People of Young and Middle Age Key Members Project” of Tianjin, the Natural Science Foundation of Tianjin (18JCYBJC30100).

Conflicts of Interest

The authors declare that they have no known competing financial interests or personal relationships that could have appeared to influence the work reported in this paper.

Ethics declarations

Not applicable

Consent to participate

All the authors (Mingshan Qin, Juan Gao, Dongwei Wei, Liuan Li, Cun Li, Linyan Yang) have agreed to report this manuscript in this paper.

Consent for publication

All the authors (Mingshan Qin, Juan Gao, Dongwei Wei, Liuan Li, Cun Li, Linyan Yang) have agreed to report this manuscript in this paper.

Availability of data and material

Raw data and materials are available on request to the author.

Code availability

Not applicable

Authors' contributions

All the authors (Mingshan Qin, Juan Gao, Dongwei Wei, Liuan Li, Cun Li, Linyan Yang) made substantial contribution while preparing the manuscript.

References

1. T. Gadzikwa, G. Lu, C.L. Stern, S.R. Wilson, J.T. Hupp, S.T. Nguyen, Covalent surface modification of a metal-organic framework: selective surface engineering via Cu^{I}-catalyzed Huisgen cycloaddition. Chem. Commun., 2008, 5493–5495
2. S. Rostamnia, H. Alamgholiloo, M. Jafari, Ethylene diamine post-synthesis modification on open metal site Cr-MOF to access efficient bifunctional catalyst for the Hantzsch condensation reaction. Appl Organometal Chem. **32**, e4370 (2018)
3. A.D. Burrows, C.G. Frost, M.F. Mahon, C. Richardson, Post-synthetic modification of tagged metal-organic frameworks. Angew. Chem. Int. Ed. **47**, 8482–8486 (2008)
4. S. Feng, Z. Ni, S. Feng, Z. Zhang, S. Liu, R. Wang, J. Hu, One-step synthesis of magnetic composite UiO-66/Fe_3O_4/GO for the removal of radioactive cesium ions. J. Radioanal. Nucl. Chem. **319**, 737–748 (2019)
5. H. Dong, G.X. Yang, X. Zhang, X.B. Meng, J.L. Sheng, X.J. Sun, Y.J. Feng, F.M. Zhang, Folic acid-functionalized Zr-based metal-organic frameworks as drug carriers for active tumor-targeted. Chemistry -A European Journal **24**, 17148–17154 (2018)
6. M.J. Ingleson, R. Heck, J.A. Gould, M.J. Rosseinsky, Nitric oxide chemisorption in a postsynthetically modified metal-organic framework. Inor. Chem. **48**, 9986–9988 (2009)

7. S.N. Kim, S.T. Yang, J. Kim, J.E. Park, W.S. Ahn, Post-synthesis functionalization of MIL-101 using diethylenetriamine: a study on adsorption and catalysis. CrystEngComm **14**, 4142–4147 (2012)
8. S. Beg, M. Rahman, A. Jain, S. Saini, P. Midoux, C. Pichon, F.J. Ahmad, S. Akhter. Nanoporous metal organic frameworks as hybrid polymer-metal composites for drug delivery and biomedical applications. Drug Discovery Today **22**, 625–637 (2017)
9. Y.K. Hwang, D.Y. Hong, J.S. Chang, S.H. Jhung, Y.K. Seo, J. Kim, A. Vimont, M. Daturi, C. Serre, G. Férey. Amine grafting on coordinatively unsaturated metal centers of MOFs: consequences for catalysis and metal encapsulation. Angew. Chem. Int. Ed. **47**, 4144–4148 (2008)
10. M.J. Katz, Z.J. Brown, Y.J. Colon, P.W. Siu, K.A. Scheidt, R.Q. Snurr, J.T. Hupp, O.K. Farha. A facile synthesis of UiO-66, UiO-67 and their derivatives. Chem. Commun. **49**(82), 9449–9451 (2013)
11. Z.G. Hu, D. Zhao, De facto methodologies toward the synthesis and scale-up production of UiO-66-type metal-organic frameworks and membrane materials. Dalton transactions **44**(44), 19018–19040 (2015)
12. L.Y. Yang, Y.P. Zhang, R. Lv, J.Yo Wang, X. Fu, W. Gu, X. Liu. Serrated single-wall metal-organic nanotubes (SWMONTs) for benzene adsorption. CrystEngComm **17**, 5625–5628 (2015)
13. W.G. Li, G. Li, D. Liu, Synthesis and application of core-shell magnetic metal-organic framework composites Fe_3O_4/IRMOF-3. RSC Adv. **6**, 94113–94118 (2016)
14. Z. Wang, J. Liu, Z. Li, X.B. Wang, P. Wang, D. Wang, F.J. Zhang, Crosslinking modification of a porous metal-organic framework (UIO-66) and hydrogen storage properties. New J. Chem. **44**, 11164–11171 (2020)
15. S. Abednatanzi, A. Abbasi, M. Masteri-Farahani, Post-synthetic modification of nanoporous $Cu_3(BTC)_2$ metal-organic framework via immobilization of a molybdenum complex for selective epoxidation. J. Mol. Catal. A: Chem. **399**, 10–17 (2015)
16. N. Andhariya, R. Upadhyay, R. Mehta, B. Chudasama, Folic acid conjugated magnetic drug delivery system for controlled release of doxorubicin. J. Nanopart. Res. **15**(1416), 1–12 (2013)
17. S. Lin, Y.F. Zhao, Y.S. Yun, Highly effective removal of nonsteroidal anti-inflammatory pharmaceuticals from water by Zr(IV)-based metal-organic framework: adsorption performance and mechanisms. ACS Appl. Mater. Interfaces **10**(33), 28076–28085 (2018)
18. W.M. Zhang, Z.M. Yan, J. Gao, P. Tong, W. Liu, L. Zhang, Metal-organic framework UiO-66 modified magnetite@silica core-shell magnetic microspheres for magnetic solid-phase extraction of domoic acid from shellfish samples. J. Chromatogr. A **1400**, 10–18 (2015)
19. Y.M. Zhang, J. Zhang, M.M. Tian et al., Fabrication of amino-functionalized Fe_3O_4@$Cu_3(BTC)_2$ for heterogeneous Knoevenagel condensation. Chin. J. Catal. **37**, 420–427 (2016)
20. G.H. Wang, Y.Q. Lei, H.C. Song, Evaluation of Fe_3O_4@SiO_2-MOF-177 as an advantageous adsorbent for magnetic solid-phase extraction of phenols in environmental water samples[J]. Anal Methods, 2014(6), 7842–7847

21. R. Kardanpour, S. Tangestaninejad, V. Mirkhani, M. Moghadamn, I. Mohammadpoor-Baltork, F. Zadehahmadi, Anchoring of Cu(II) onto surface of porous metal-organic framework through post-synthesis modification for the synthesis of benzimidazoles and benzothiazoles. J. Solid State Chem. **235**, 145–153 (2016)
22. M.A. Gotthardt, A. Beilmann, R. Schoch, J. Engelke, W. Kleist, Post-synthetic immobilization of palladium complexes on metal-organic frameworks-a new concept for the design of heterogeneous catalysts for Heck reactions. RSC Adv. **3**, 10676–10679 (2013)
23. G. Xiong, X.L. Chen, L.X. You, B.Y. Ren, F. Ding, I. Dragutan, V. Dragutan, Y.G. Sun, La-metal-organic framework incorporating Fe_3O_4 nanoparticles, post-synthetically modified with Schiff base and Pd. A highly active, magnetically recoverable, recyclable catalyst for CAC cross-couplings at low Pd loadings. J. Catal. **361**, 116–125 (2018)

Figures

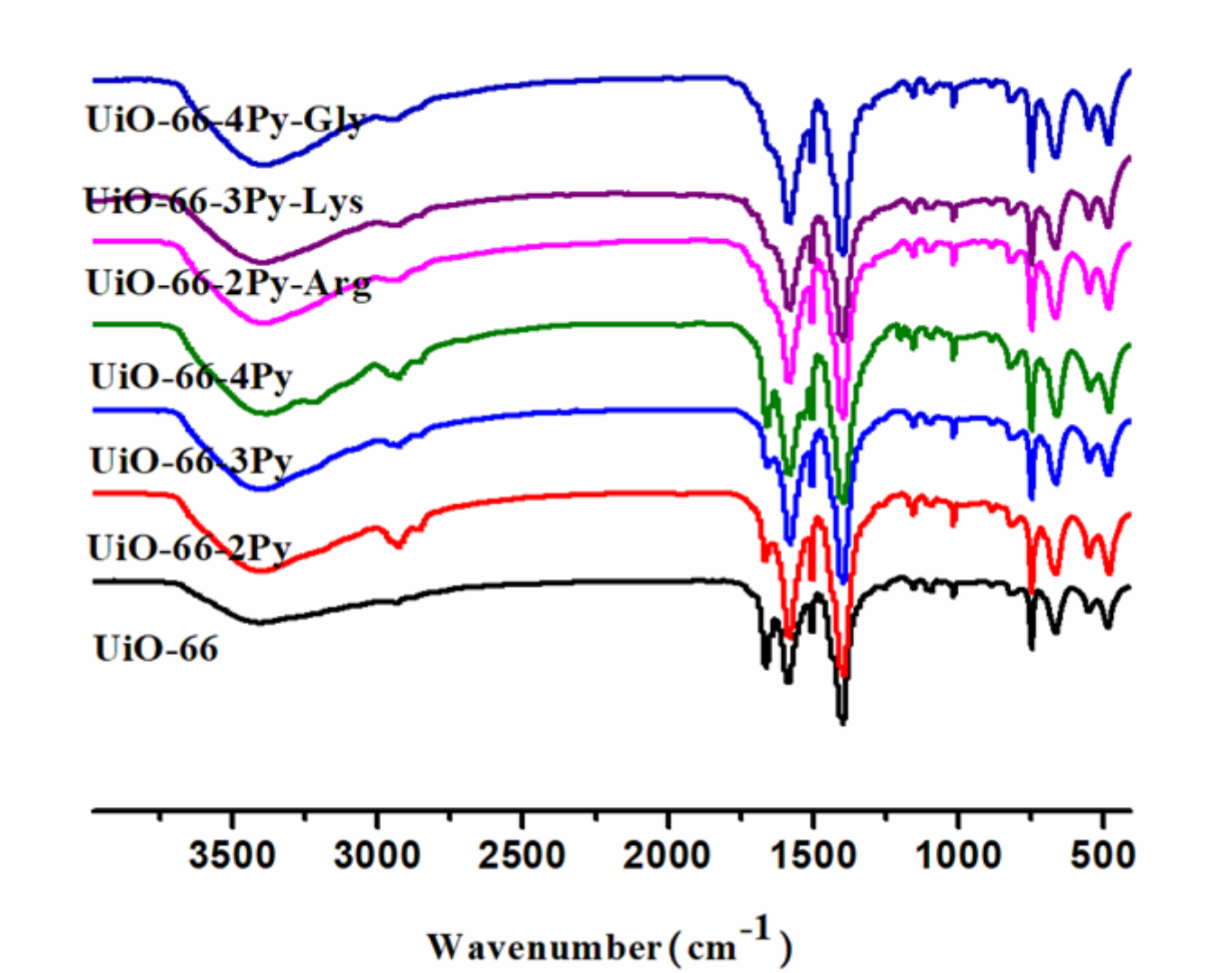

Figure 1

IR spectra of UiO66 nanoparticles(black), UiO66-2Py nanoparticles(red), UiO66-3Py nanoparticles(blue), UiO66-4Py nanoparticles(green), UiO66-2Py-Arg nanoparticles(pink), UiO66-3Py-Lys nanoparticles(purple), UiO66-4Py-Gly(Navy blue).

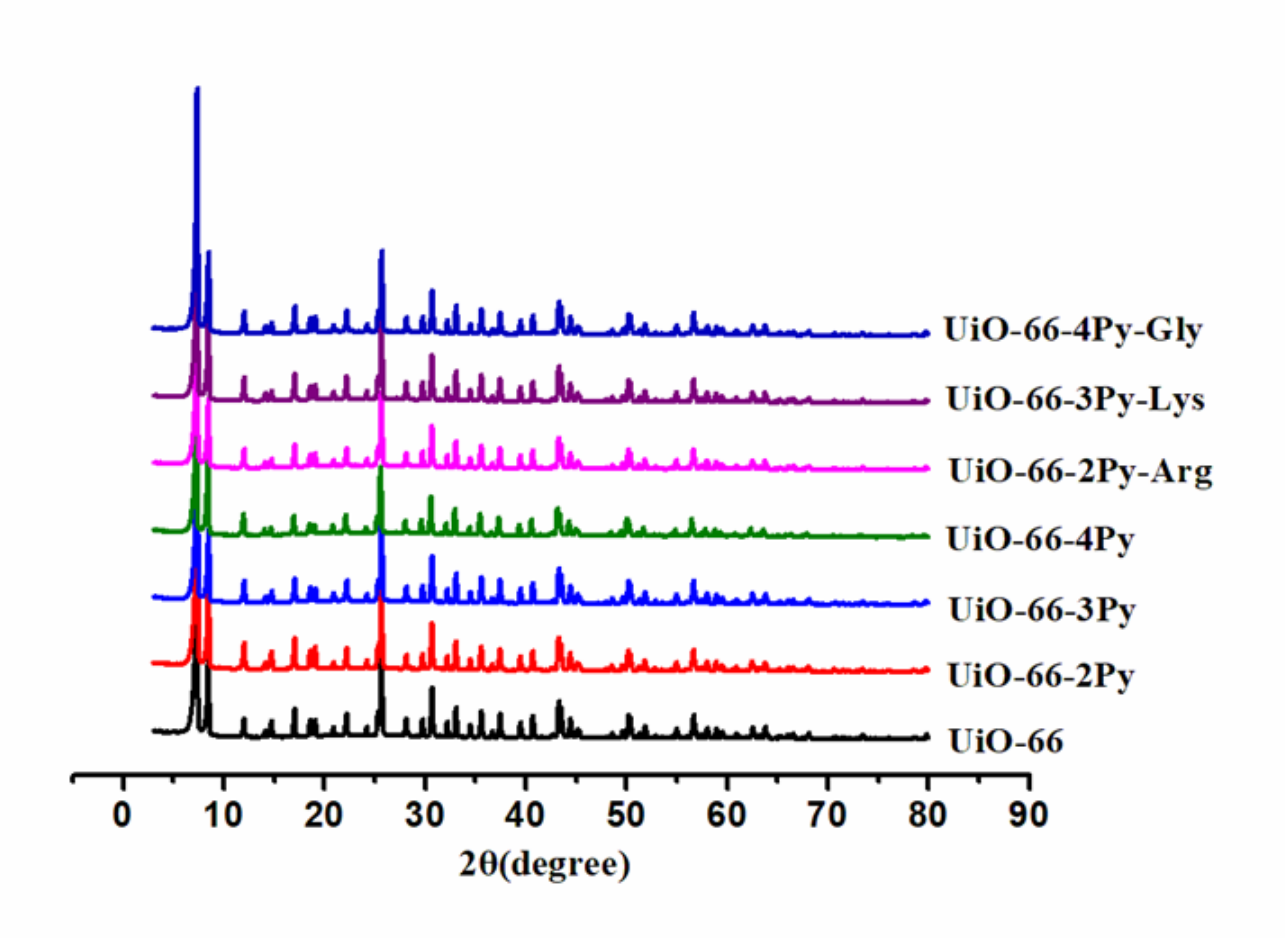

Figure 2

XRD pattern of UiO66 (black), UiO66-2Py (red), UiO66-3Py (blue), UiO66-4Py (green), UiO66-2Py-Arg (pink), UiO66-3Py-Lys (purple), UiO66-4Py-Gly (Navy blue).

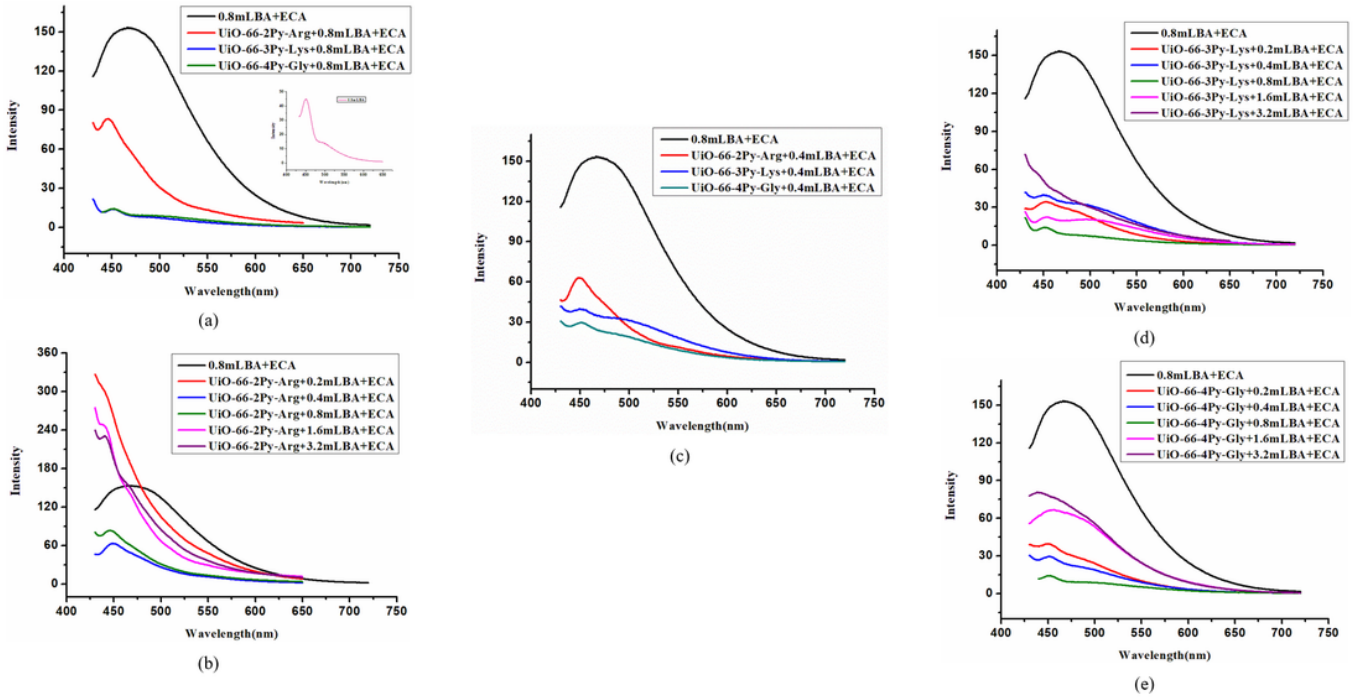

Figure 3

(a) The fluorescence intensity of the catalytic reaction solution of UiO66-2Py-Arg, UiO66-3Py-Lys and UiO66-4Py-Gly under the volume of 0.8mL benzaldehyde, (b) the fluorescence intensity of UiO66-2Py-Arg catalytic reaction solution, (c) The fluorescence intensity of the catalytic reaction solution of UiO66-2Py-Arg, UiO66-3Py-Lys and UiO66-4Py-Gly under the volume of 0.4mL benzaldehyde, (d) the fluorescence intensity of the catalytic reaction solution of UiO66-3Py-Lys, (e) Fluorescence intensity of UiO66-4Py-Gly catalytic reaction solution.

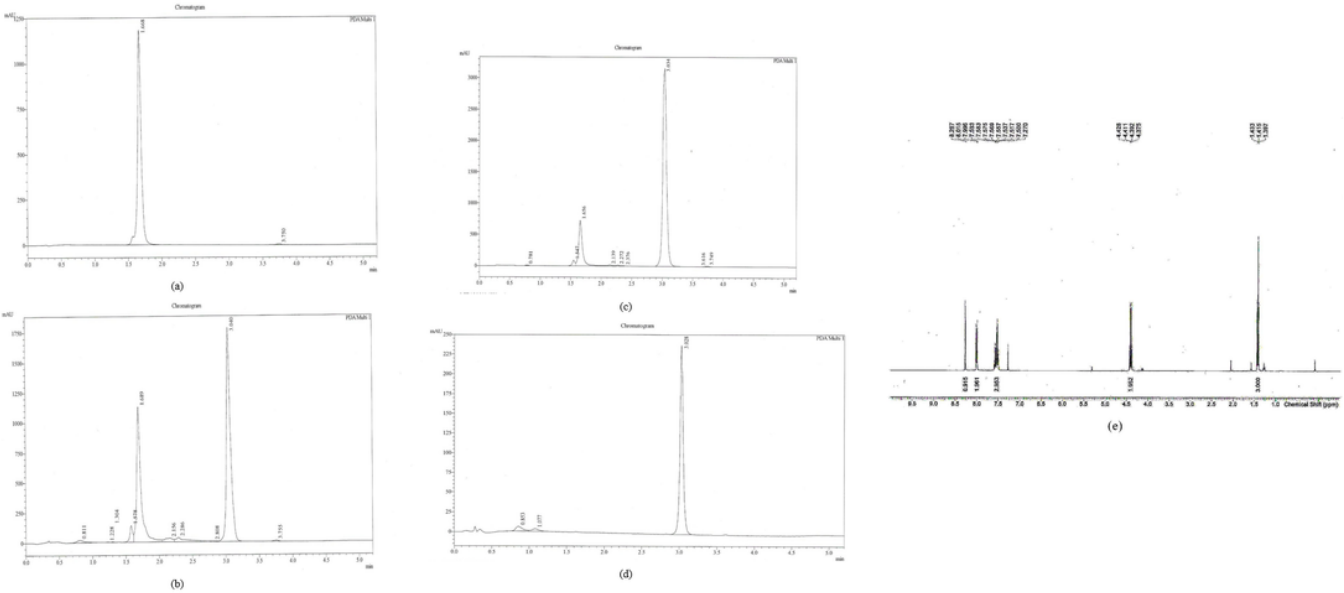

Figure 4

(a) HPLC charomatogram of benzaldehyde(220nm), (b) HPLC charomatogram of the reaction solution without catalysts(220nm), (c) HPLC charomatogram of the reaction solution catalyzed by UiO66-4Py-Gly nanoparticles(220nm), (d) HPLC charomatogram of the product(220nm), (e) 1HNMR charomatogram of the reaction product.